Current Biology 20, 374–380, February 23, 2010 ©2010 Elsevier Ltd All rights reserved DOI 10.1016/j.cub.2009.12.049

Report

The Kinesin-8 Kif18A Dampens Microtubule Plus-End Dynamics

Yaqing Du,[1] Chauca A. English,[1] and Ryoma Ohi[1,*]
[1]Department of Cell and Developmental Biology, Vanderbilt University School of Medicine, 465 21st Avenue South, Nashville, TN 37232-8240, USA

Summary

Motility is a fundamentally important property of most members of the kinesin superfamily, but a rare subset of kinesins are also able to alter microtubule dynamics. At kinetochore-microtubule plus ends, the kinesin-8 family member Kif18A is essential to align mitotic chromosomes at the spindle equator during cell division, but how it accomplishes this function is unclear. We report here that Kif18A is a plus-end-directed motor that inhibits the polymerization dynamics of microtubule plus ends without destabilizing them, distinguishing Kif18A from the budding yeast ortholog Kip3. In interphase cells, Kif18A uses this activity to reduce the overall dynamicity of microtubule plus ends and effectively constrains the distance over which plus ends grow and shrink. Our findings suggest that kinesin-8 family members have developed biochemically distinct activities throughout evolution and have implications for how Kif18A affects kinetochore-microtubule plus-end dynamics during mitosis in animal cells.

Results and Discussion

At kinetochore-microtubule (MT) plus ends, kinesin-8 motors help to align mitotic chromosomes to the metaphase plate [1–7]. In human cells, depletion of the kinesin-8 Kif18A causes a prometaphase arrest, where chromosomes misalign as a result of abnormally persistent oscillations [4, 5, 7]. In vitro, some kinesin-8s (e.g., budding yeast Kip3) are plus-end-directed motors that destabilize MT plus ends in a manner similar to kinesin-13s [4, 8, 9]. This has led to a model in which Kif18A preferentially concentrates on MT plus ends attached to a lagging kinetochore and causes the chromosome to reverse its direction of movement by destabilizing lagging kinetochore-MTs [5]. The generality of this mechanism is unclear, however, because other kinesin-8s (e.g., fission yeast Klp5/6) do not depolymerize MTs [10] despite having a common function in mitosis.

To investigate how Kif18A influences chromosome movements, we expressed and purified full-length Kif18A protein (Figure 1A). In gliding assays [11], polarity-marked MTs assembled with the slowly hydrolyzed GTP analog GMPCPP were translocated by Kif18A in an ATP-dependent manner with their minus ends leading (Figure 1B). This indicates that Kif18A is a plus-end-directed kinesin. At high coverslip surface densities, MTs moved at 6.2 ± 0.18 μm/min (mean ± standard error of the mean [SEM]; n = 52) (Figure 1C). We conclude that our purified Kif18A is an active molecular motor and that Kif18A is a faster plus-end-directed kinesin than previously reported [4].

At low motor concentrations (25 nM), we observed many MTs to be thermally pivoting, bound to the coverslip via a single attachment point for extended periods. Time-lapse imaging revealed that MTs moved with their minus ends leading until the motor reached the plus ends, at which point pivoting initiated (Figure 1D). We quantified the dwell time at MT plus ends by measuring how long MTs pivoted before they dissociated from the coverslip. The kinetics of MT dissociation were fit by a single exponential yielding a dissociation rate constant of 0.013 s^{-1}. Our analysis suggests that, similar to the budding yeast kinesin-8 Kip3 [9, 12], Kif18A pauses once it translocates to MT plus ends.

Because Kif18A and Kip3 have been reported to depolymerize GMPCPP MTs [4, 8, 9], we were surprised that MTs were not destabilized in our motility assays. We examined this further by comparing the abilities of Kif18A and the kinesin-13 MCAK [13] to depolymerize GMPCPP MTs (1 μM tubulin) attached to a coverslip. Although 25 nM MCAK efficiently depolymerized GMPCPP MTs at 1.17 ± 0.06 μm/min (mean ± SEM; n = 32), MTs were stable even in the presence of high (250 nM) Kif18A concentrations (Figures 2A and 2B); depolymerization rates of MTs in the presence of Kif18A (0.033 ± 0.006 μm/min; n = 32) were similar to those of control MTs (0.03 ± 0.003 μm/min; n = 32). Comparable results were obtained with paclitaxel-stabilized MTs (see Figure S1A available online).

Although Kif18A might not destabilize GMPCPP MTs, we reasoned that plus-end-attached Kif18A might affect MT assembly. To test this, we used GMPCPP MT seeds (red) to nucleate the assembly of GTP-tubulin (green), producing two-colored MTs (Figure 2C, −Kif18A). When Kif18A was present during the polymerization reaction, even at levels highly substoichiometric to tubulin (150 nM motor:15 μM tubulin), Kif18A blocked formation of red:green MTs, and in their place were red seeds that were capped with green fluorescence (Figure 2C, +Kif18A). This result suggests that Kif18A either prevents the assembly of GTP tubulin or depolymerizes GTP MTs once they have formed.

To distinguish between these possibilities, we polymerized GTP MTs off of axonemes and varied the time of Kif18A addition (Figure 2D). If Kif18A prevents polymerization by blocking plus-end assembly, the motor should not affect MT stability once filaments have formed. In contrast, if Kif18A is a depolymerase, MTs should be destabilized regardless of when motor is added. In the absence of motors, MTs grew from both axoneme ends, but their lengths differed (Figures 2E and 2F; n = 194), with long (10 μm) MTs extending off of plus ends and short (3 μm) MTs extending off of minus ends. To avoid end bias in quantifying our data, we measured the lengths of equal numbers of MTs off of each axoneme end. As expected for a depolymerase, MCAK suppressed MT assembly off of axonemes irrespective of the time of addition [14]. When Kif18A was present during the polymerization reaction, MT assembly was inhibited, with short MTs averaging 1.4 μm and long MTs averaging 3.5 μm (n = 200). In contrast to MCAK, Kif18A had little effect on MT length (long end 13 μm,

*Correspondence: ryoma.ohi@vanderbilt.edu

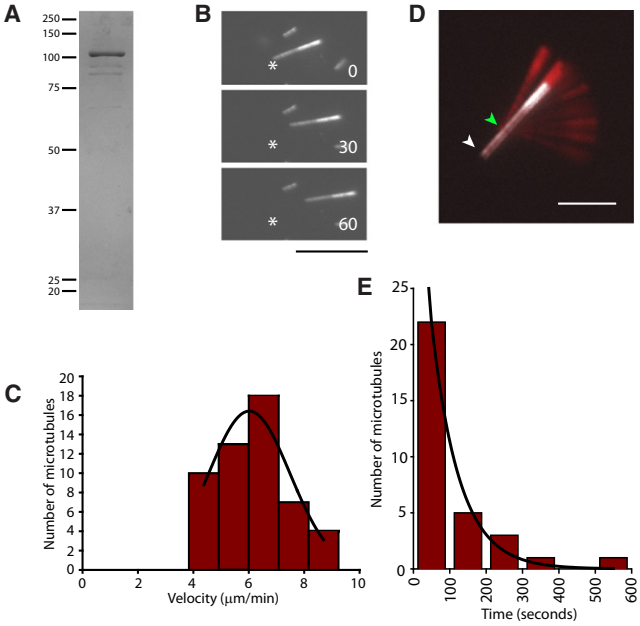

Figure 1. Kif18A Is a Plus-End-Directed Motor that Pauses at Microtubule Plus Ends

(A) Purification of recombinant Kif18A. Coomassie blue-stained gel of 1 μg purified motor is shown.

(B) Kif18A is a plus-end-directed motor. Images from a time-lapse sequence of a Kif18A motility assay with bright/dim (minus end/plus end) GMPCPP microtubules (MTs) are shown. Asterisk denotes fixed reference point. Time is indicated in seconds. Scale bar represents 5 μm.

(C) MT gliding velocities. Motility assays were performed with a high surface density of Kif18A, and the velocities of MT gliding were quantified (n = 52). The black line is a fit of the data to a Gaussian distribution.

(D) Kif18A pauses at MT plus ends. Shown are superimposed images from a 390 s time-lapse sequence of a MT gliding at low Kif18A surface density. The MT is pseudocolored white at t = 0 and red at subsequent time points. In this sequence, the MT slides a short distance (designated by the white [t = 0] and green arrowheads) before ceasing movement and initiating nodal pivoting. Time step between frames is 5 s. Scale bar represents 2 μm. See also Movie S1.

(E) Histogram of the lengths of time that MTs remain attached to the coverslip upon initiation of thermal pivoting (n = 32 MTs). The black line is a single-exponential fit of the data that gives a dissociation rate constant of 0.013 s^{-1}.

short end 2.8 μm; n = 184) if it was added after polymerization was allowed to occur (Figures 2E and 2F), indicating that Kif18A does not destabilize GTP MTs.

To determine whether Kif18A antagonizes MT growth off of one end or both, we localized Kif18A on axonemes by supplementing reactions with Kif18A antibodies (Figures S1B and S1C) 4 min prior to fixation. Under these conditions, ~70% of axonemes (n = 103) exhibited bright fluorescence at one end, whereas axonemes in reactions lacking Kif18A showed only background fluorescence (Figure 2G). Quantitation of MT lengths indicated that Kif18A specifically affects the length of MTs grown off of axoneme plus ends (Figure 2H). Ends lacking Kif18A staining were 3.0 μm (n = 84), similar to short MTs in control reactions (2.92 μm; n = 61), and MTs associated with Kif18A-positive axoneme ends were stunted (1.4 μm; n = 84) compared to long MTs (7.9 μm; n = 61) assembled in control reactions. These results indicate that Kif18A antagonizes MT polymerization specifically at the plus end.

We next investigated whether Kif18A suppresses MT polymerization dynamics in vivo. MT density within the mitotic spindle makes it challenging to measure plus-end dynamics of single kinetochore-MTs. Thus, we engineered a mutant, Kif18A.NLS^{mut}, which is cytoplasmic during interphase so that its effect on individual interphase MTs could be analyzed. We mapped a monopartite nuclear localization sequence (NLS) (K^{828}RKRK) to the tail domain of Kif18A (Figure 3A) and mutated the charged residues to alanines to generate Kif18A.NLS^{mut} (Figure 3B).

In contrast to wild-type Kif18A, which localized to nuclei during interphase, Kif18A.NLS^{mut} exhibited a punctate cytoplasmic distribution in HeLa cells and accumulated at the cell periphery (Figure 3C). Double labeling of transfected cells with tubulin antibodies revealed that Kif18A localized predominantly to MT tips. We used the Kif18A NLS mutant in an in vivo MT depolymerization assay [15] to test whether Kif18A disassembles interphase MTs. We found that Kif18A.NLS^{mut}, unlike MCAK, does not destabilize cytoplasmic MTs when overexpressed (Figures 3D and 3E). Tubulin fluorescence intensities in fixed Kif18A.NLS^{mut}-transfected cells were similar to those in control cells and were reduced ~2-fold in the presence of similar cytoplasmic levels of MCAK as judged by GFP fluorescence (Figure 3E). This result is consistent with the lack of observed depolymerization activity in vitro.

Collectively, these data suggest that Kif18A is not a MT depolymerase but rather functions by antagonizing MT plus-end assembly dynamics. To examine how Kif18A affects MT disassembly/assembly in cells, we expressed Kif18A.NLS^{mut} in HeLa cells (Figure S2A) and examined MTs in interphase cells exposed to cold and following recovery from nocodazole treatment. In cold-treated cells, MT disassembly was qualitatively similar in control and transfected cells (Figure S2B), suggesting that the motor does not grossly stabilize MT plus ends. To test whether Kif18A blocks MT assembly, we used a nocodazole washout assay. HeLa cells transfected with Kif18A.NLS^{mut} were treated with nocodazole and analyzed by tubulin immunofluorescence following drug removal. Although MTs had formed 10 min after nocodazole washout in untransfected cells, MT assembly was blocked in Kif18A.NLS^{mut}-positive cells (Figures 4A and 4B), suggesting that Kif18A is able to suppress MT assembly in vivo.

To examine the effect of Kif18A on the dynamics of polymerized MTs, we introduced Kif18A.NLS^{mut} into LLCPK1 cells stably expressing GFP-α-tubulin (LLCPK1α; [16]) and imaged MT dynamics by time-lapse microscopy. Interestingly, Kif18A.NLS^{mut} often localized to a subset of interphase MTs (Figure 4C). The significance of these localizations is unclear, but they could arise from cooperativity in motor-MT interactions or Kif18A recruitment to a specific population of MTs. We restricted our analysis of MT dynamics to those filaments that were visibly bound to Kif18A protein (Movies S4 and S5). Still images of peripherally located MTs in control and Kif18A.NLS^{mut}-transfected cells are shown in Figure 4D. As expected [16], MTs alternated between phases of growth (green arrowhead) and shrinkage (red arrowhead) and exhibited periods where MTs paused and showed little change (<0.5 μm) in length.

To measure the parameters of MT dynamic instability, we generated life history plots of individual MTs (Figure 4E). Comparison of the parameters revealed that MTs were 25% less dynamic in cells expressing Kif18A.NLS^{mut} (Table 1). This reduction in dynamicity was due to subtle and complex changes in multiple parameters. Most notably, the space traversed and time spent during individual MT growth and shortening phases were reduced; growth and shrinkage

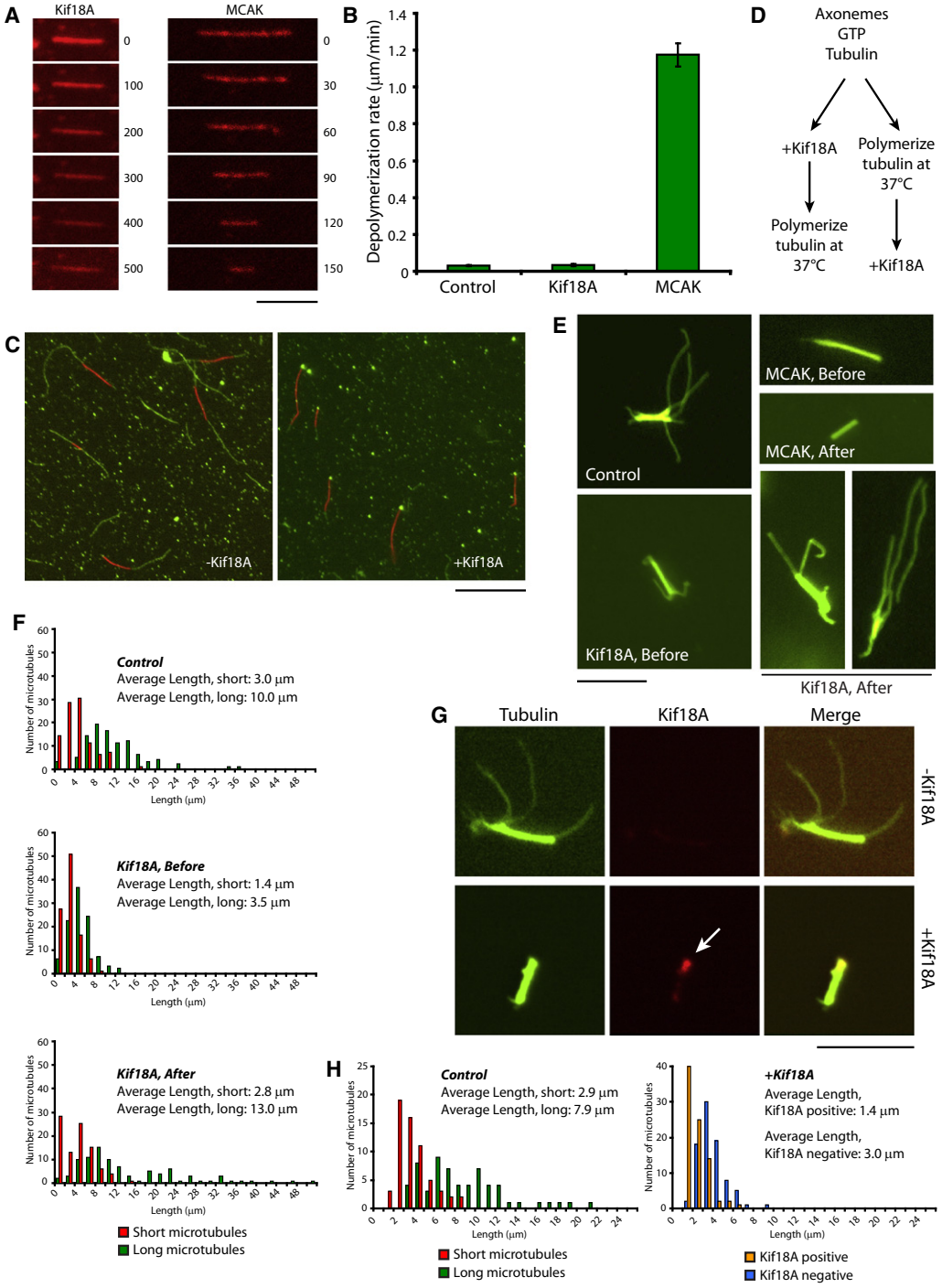

Figure 2. Kif18A Blocks GTP-Tubulin Assembly

(A) Kif18A does not depolymerize GMPCPP MTs. Representative images from time-lapse sequences of GMPCPP MTs in the presence of 250 nM Kif18A and 25 nM MCAK are shown. Time is indicated in seconds. Scale bar represents 5 μm. See also Movies S2 and S3.

(B) Mean depolymerization rates (± standard error of the mean [SEM]) of GMPCPP MTs in the absence of motor, in the presence of 250 nM Kif18A, and in the presence of 25 nM MCAK (n = 32 per condition).

(C) Kif18A prevents GTP tubulin assembly. Alexa 488-labeled GTP-tubulin (green) was elongated off of rhodamine-labeled GMPCPP MTs (red) to generate red:green MTs of mixed nucleotide composition. Buffer (−Kif18A) or motor (+Kif18A; 150 nM) was added to the reaction prior to polymerization at 37°C. Scale bar represents 10 μm.

(D) Design of the experiment presented in (E) and (F).

(E) Kif18A blocks GTP-tubulin assembly off of axonemes without destabilizing MTs. Axonemes were incubated with 15 μM tubulin at 37°C in the presence of buffer (control), MCAK (250 nM), or Kif18A (250 nM), sedimented onto coverslips, and stained for tubulin. MCAK and Kif18A were added either before or after tubulin assembly. Scale bar represents 5 μm.

(F) Quantitation of axonemal MT lengths from (E). Histograms depict length distribution of MTs binned into either short (red) or long (green) categories ($n \geq 200$ per condition from 2–3 independent experiments).

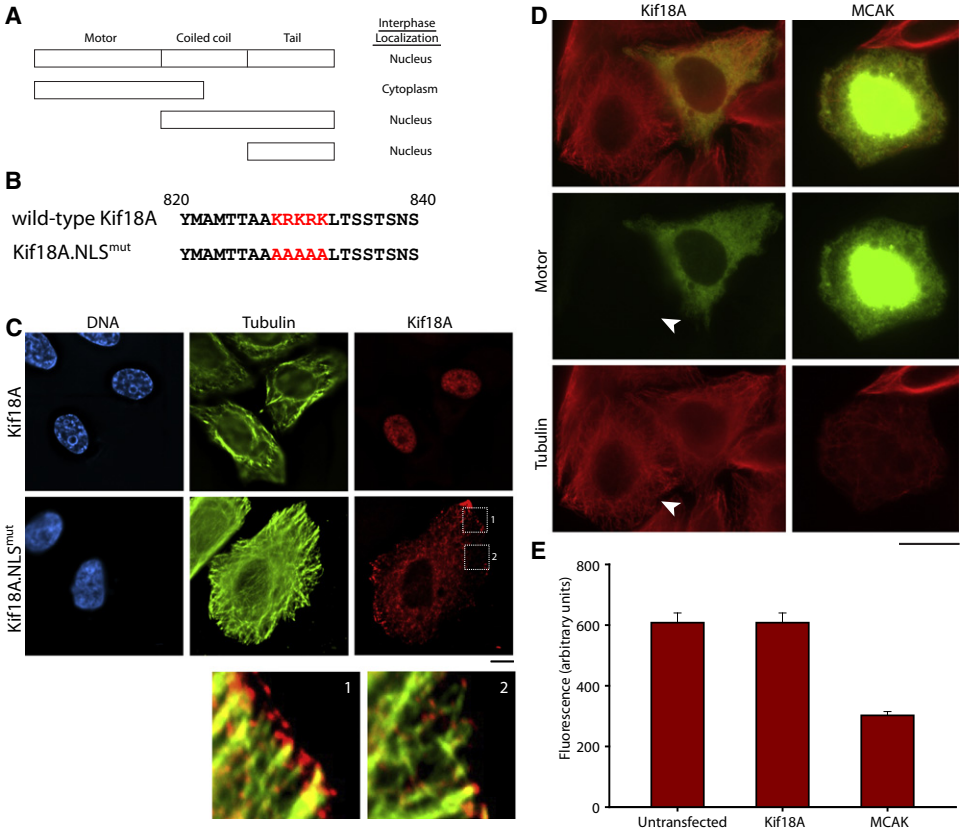

Figure 3. Engineering a Constitutively Cytoplasmic Kif18A Mutant

(A) Mapping of the Kif18A nuclear localization sequence (NLS). The indicated regions of Kif18A were fused to GFP and localized in interphase HeLa cells.

(B) Identification of the Kif18A NLS. Positively charged Kif18A tail residues (828–832) that conform to a canonical NLS are highlighted in red. The primary sequence of Kif18A.NLS^{mut}, with altered residues indicated in red, is shown below the wild-type sequence.

(C) Kif18A.NLS^{mut} is cytoplasmic during interphase. Cherry-fused wild-type or Kif18A.NLS^{mut} proteins were localized in HeLa cells and coimaged with tubulin. Boxed regions in the Kif18A.NLS^{mut}-transfected cell are enlarged in boxes 1 and 2 at bottom to emphasize MT tip localization of Kif18A.NLS^{mut}. Scale bar represents 10 μm.

(D) Kif18A.NLS^{mut} does not destabilize cytoplasmic MTs. HeLa cells were transfected with constructs expressing GFP-MCAK or GFP-Kif18A.NLS^{mut}, fixed, and stained with tubulin antibodies. Arrowhead indicates an untransfected cell. Scale bar represents 20 μm.

(E) Quantitation of MT stability in cells expressing Kif18A.NLS^{mut} and MCAK ($n \geq 50$ cells per condition; error bars show SEM).

distances were decreased by 17% and 33%, respectively, and the durations of each phase decreased by ~12%. Modest increases in the frequencies of both catastrophes (14%) and rescues (11%) were also observed, suggesting that Kif18A causes MTs to interconvert between growth and shrinkage more frequently. Finally, although Kif18A did not affect the frequency of MT pausing, Kif18A did cause MTs to pause 26% longer. Collectively, our data indicate that Kif18A acts as a damper, constraining the distance over which plus ends grow and shrink, and suggest that Kif18A utilizes this mechanism to regulate the dynamics of kinetochore-MTs during cell division.

Bipolar spindle assembly is sensitive to changes in MT dynamics [17]. For example, disruption of MT dynamics by drugs (e.g., taxanes) or removal of protein factors that regulate MT assembly (e.g., XMAP215/chTOG) induces multipolar spindle formation. Because Kif18A attenuates MT assembly dynamics in vitro and in cells, we examined the effect of Kif18A overexpression on spindle assembly. Overexpression of GFP-Kif18A in HeLa cells caused a 7-fold increase in the number of mitotic cells containing multipolar spindles (35.2 ± 10.7%, mean ± standard deviation; n = 130) compared to GFP-expressing control cells (5.1 ± 1.9%; n = 228; Figures 4G and 4H). Thus, high levels of Kif18A block both chromosome movements [5] and spindle assembly, presumably by altering MT polymerization dynamics.

Overall, our findings suggest that Kif18A contributes to chromosome congression through a depolymerase-independent mechanism [5]. In interphase cells, Kif18A affected multiple parameters of MT dynamics, but its ability to reduce the persistence of MT growth and shortening phases is the most intriguing because Kif18A also restricts the directional persistence of kinetochores during mitosis [5]. Because kinetochore-MT dynamics underlie kinetochore movements [18, 19], we speculate that the effect of Kif18A on individual kinetochore-MTs translates to a similar effect on kinetochore

(G) Localization of Kif18A on axonemes. Regrown axonemes in the presence (+Kif18A) and absence (−Kif18A) of Kif18A were spiked with fluorescently labeled Kif18A antibodies, fixed, and stained with antibodies against tubulin. The arrow indicates bright Kif18A staining at one axoneme end. Scale bar represents 10 μm.

(H) Quantitation of axonemal MT lengths from (G). MTs for the control experiment were quantified as in (F). MT lengths for Kif18A-decorated axonemes were quantified as a function of Kif18A staining: orange represents positive staining; blue represents lack of staining.

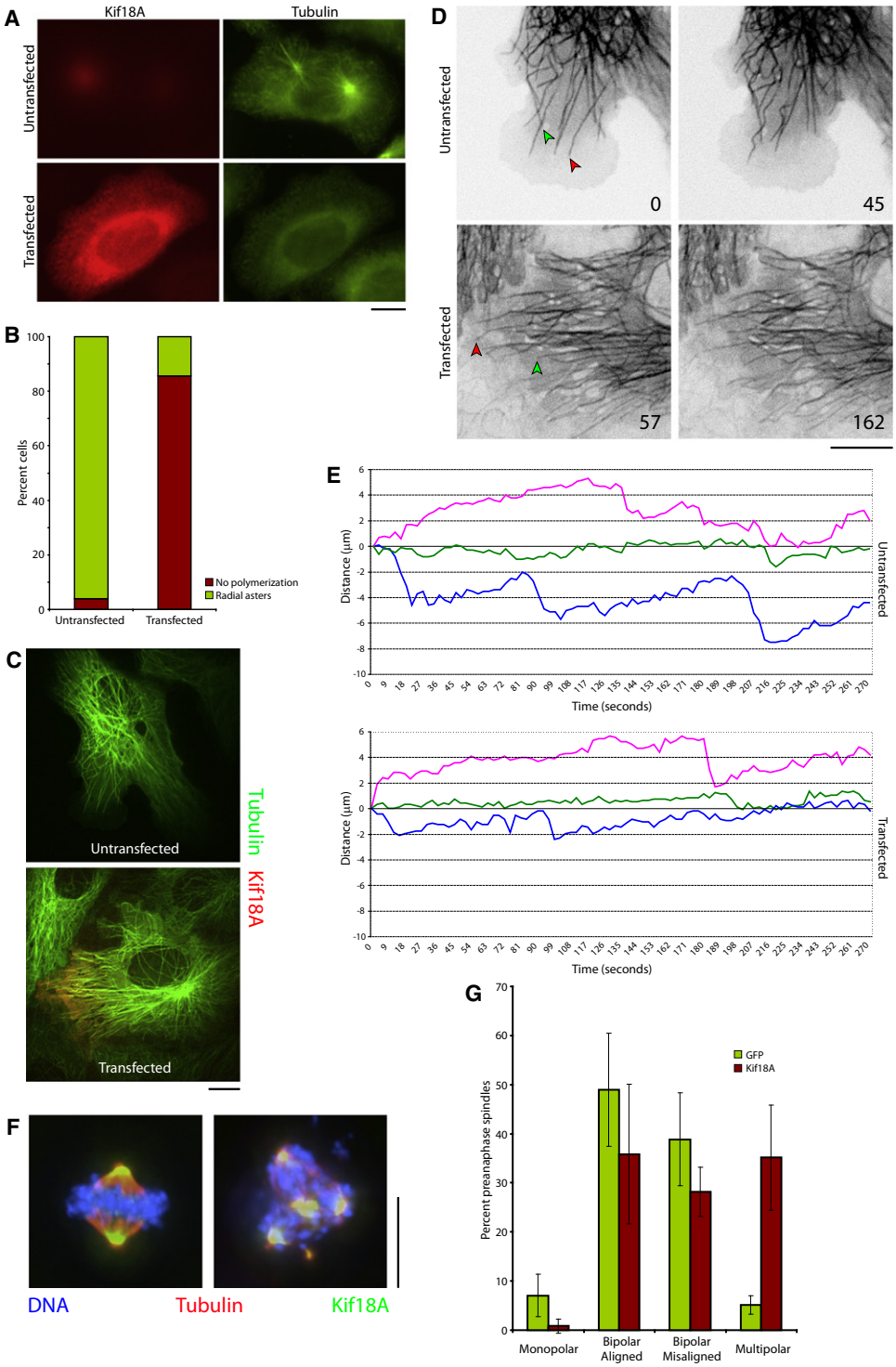

Figure 4. Kif18A Inhibits the Dynamic Instability of Interphase MTs

(A) Kif18A antagonizes MT regrowth upon nocodazole washout. Images of MTs in untransfected or Kif18A.NLS^{mut}-transfected HeLa cells 10 min following nocodazole washout are shown. Scale bar represents 10 μm.

(B) Quantitation of cells containing MTs from the experiment in (A) ($n \geq 200$ per condition).

(C) Two-color images of untransfected and Kif18A.NLS^{mut}-transfected LLCPK1α cells. Scale bar represents 10 μm. See also Movies S4 and S5.

(D) Still images depicting MT dynamics in untransfected and Kif18A.NLS^{mut}-transfected LLCPK1α cells. Red arrowheads denote shortening MTs; green arrowheads point to polymerizing MTs. Time in seconds is indicated at the lower right of each panel. Scale bar represents 10 μm.

(E) Life history plots of individual MTs. Not all MTs chosen here are from the cells shown in (D). The scale is identical for each plot.

(F) Kif18A overexpression causes multipolar spindle formation. Shown are images of mitotic GFP-Kif18A-transfected cells that contain bipolar and multipolar spindles. Scale bar represents 10 μm.

(G) Quantitation of preanaphase spindle morphologies in cells overexpressing Kif18A. The percentages of phenotypes observed are averaged from three independent experiments (n = 228, GFP-transfected cells; n = 130, GFP-Kif18A transfected cells). Error bars show standard deviation.

Table 1. Quantitation of Microtubule Dynamics in Kif18A.NLS^{mut}-Transfected Cells

Dynamic Parameter	Untransfected Cells (67 Microtubules)	Kif18A.NLS^{mut}-Transfected Cells (51 Microtubules)
Growth rate (μm/s)	0.146 ± 0.004	0.154 ± 0.007
Growth distance (μm)	1.10 ± 0.04	0.91 ± 0.03
Growth duration (s)	10.58 ± 0.56	9.25 ± 0.53
Shrinkage rate (μm/s)	0.269 ± 0.010	0.235 ± 0.011
Shrinkage distance (μm)	2.02 ± 0.14	1.36 ± 0.09
Shrinkage duration (s)	7.78 ± 0.37	6.87 ± 0.39
Average pause duration (s)	18.12 ± 0.85	22.76 ± 1.47
Percent time per phase (growth/shrinkage/pause)	28.5/12.5/59.0	22.1/12.5/65.3
Rescue frequency (s^{-1})	0.132	0.146
Catastrophe frequency (s^{-1})	0.021	0.024
Pause frequency (s^{-1})	0.033	0.029
Dynamicity (dimer/s)	105	79

Values are given as mean ± standard error of the mean.

oscillations. That Kif18A is a mild regulator of MT dynamics in vivo may be well suited to its function in kinetochore-MT regulation. Kinetochore movements in vertebrates reflect the integrated dynamics of ~30 MTs [20], and small changes in the dynamics of individual MTs are likely to be significant.

Generally, the effects of Kif18A, *Schizosaccharomyces pombe* Klp5/6 [21], and budding yeast Kip3 [8] on MT dynamics appear similar (Table S1). Rescue and catastrophe frequencies are elevated to varying degrees by all three motors [8, 21], and the durations of MT growth and shortening phases are lengthened in *kip3*Δ cells [8]. Thus, all kinesin-8s reduce the persistence of MT growth and shrinkage phases. Data supporting a role for kinesin-8s in destabilizing MTs in vivo are less compelling. Klp5/6 and Kip3 strongly reduce MT dwell times at cell poles by destabilizing MT tips that contact the cell cortex [8, 22], but other biochemical or mechanical factors might synergize with Kip3 or Klp5/6 to catalyze this effect [22].

Given that Kip3, Klp5/6, and Kif18A similarly affect MT dynamics in cells, why is Kip3 unique in its ability to destabilize MTs in vitro? At MT plus ends, Kip3 tightly associates with the terminal tubulin subunit and removes it when a trailing Kip3 molecule displaces the motor-tubulin complex [12]. It is possible that Kif18A and Klp5/6 interact more weakly with dimers at plus ends and that their displacement by incoming motors does not cause dimer removal. A second possibility, suggested by our finding that Kif18A antagonizes GTP MT assembly, is that kinesin-8s affect MT dynamics through a second mechanism that does not involve MT depolymerization. We propose that, like XKlp1/Kif4 [23], kinesin-8s act at or near MT plus ends (i.e., on the lattice), inducing conformational changes that attenuate MT dynamic instability. Comparative analysis of how different kinesin-8s affect MT end and lattice structures will allow a formal test of these ideas.

Supplemental Information

Supplemental Information includes two figures, one table, Supplemental Experimental Procedures, and five movies and can be found with this article online at doi:10.1016/j.cub.2009.12.049.

Acknowledgments

We thank P. Chang, K. Gould, A. Groen, I. Kaverina, M. Ohi, M. Tyska, and R. Coffey for insightful discussions and critical review of the manuscript. We are grateful to J. Stumpff and L. Wordeman for sharing unpublished observations and M. Tyska for assistance with data analysis. We also thank an anonymous reviewer for raising insightful points regarding our analysis of microtubule dynamics. L. Wordeman, P. Chang, I. Kaverina, and N. Watanabe kindly provided pEGFP-MCAK, LLCPK1α cells, pmCherry-C1, and HeLa "Kyoto" cells, respectively. This work was supported by funds from the Department of Cell and Developmental Biology at Vanderbilt University, the Vanderbilt-Ingram Cancer Center, and the Robert J. and Helen C. Kleberg Foundation; pilot project grant 5P50 CA095103-07 within the National Cancer Institute Specialized Program of Research Excellence in Gastrointestinal Cancers; and American Cancer Society Institutional Research Grant IRG-58-009-49 to R.O.

Received: June 2, 2009
Revised: December 1, 2009
Accepted: December 21, 2009
Published online: February 11, 2010

References

1. Gandhi, R., Bonaccorsi, S., Wentworth, D., Doxsey, S., Gatti, M., and Pereira, A. (2004). The Drosophila kinesin-like protein KLP67A is essential for mitotic and male meiotic spindle assembly. Mol. Biol. Cell *15*, 121–131.
2. Garcia, M.A., Koonrugsa, N., and Toda, T. (2002). Two kinesin-like Kin I family proteins in fission yeast regulate the establishment of metaphase and the onset of anaphase A. Curr. Biol. *12*, 610–621.
3. Goshima, G., and Vale, R.D. (2003). The roles of microtubule-based motor proteins in mitosis: Comprehensive RNAi analysis in the Drosophila S2 cell line. J. Cell Biol. *162*, 1003–1016.
4. Mayr, M.I., Hümmer, S., Bormann, J., Grüner, T., Adio, S., Woehlke, G., and Mayer, T.U. (2007). The human kinesin Kif18A is a motile microtubule depolymerase essential for chromosome congression. Curr. Biol. *17*, 488–498.
5. Stumpff, J., von Dassow, G., Wagenbach, M., Asbury, C., and Wordeman, L. (2008). The kinesin-8 motor Kif18A suppresses kinetochore movements to control mitotic chromosome alignment. Dev. Cell *14*, 252–262.
6. West, R.R., Malmstrom, T., and McIntosh, J.R. (2002). Kinesins klp5(+) and klp6(+) are required for normal chromosome movement in mitosis. J. Cell Sci. *115*, 931–940.
7. Zhu, C., Zhao, J., Bibikova, M., Leverson, J.D., Bossy-Wetzel, E., Fan, J.B., Abraham, R.T., and Jiang, W. (2005). Functional analysis of human microtubule-based motor proteins, the kinesins and dyneins, in mitosis/cytokinesis using RNA interference. Mol. Biol. Cell *16*, 3187–3199.
8. Gupta, M.L., Jr., Carvalho, P., Roof, D.M., and Pellman, D. (2006). Plus end-specific depolymerase activity of Kip3, a kinesin-8 protein, explains its role in positioning the yeast mitotic spindle. Nat. Cell Biol. *8*, 913–923.
9. Varga, V., Helenius, J., Tanaka, K., Hyman, A.A., Tanaka, T.U., and Howard, J. (2006). Yeast kinesin-8 depolymerizes microtubules in a length-dependent manner. Nat. Cell Biol. *8*, 957–962.
10. Grissom, P.M., Fiedler, T., Grishchuk, E.L., Nicastro, D., West, R.R., and McIntosh, J.R. (2009). Kinesin-8 from fission yeast: A heterodimeric, plus-end-directed motor that can couple microtubule depolymerization to cargo movement. Mol. Biol. Cell *20*, 963–972.
11. Cohn, S.A., Saxton, W.M., Lye, R.J., and Scholey, J.M. (1993). Analyzing microtubule motors in real time. Methods Cell Biol. *39*, 75–88.
12. Varga, V., Leduc, C., Bormuth, V., Diez, S., and Howard, J. (2009). Kinesin-8 motors act cooperatively to mediate length-dependent microtubule depolymerization. Cell *138*, 1174–1183.
13. Moore, A., and Wordeman, L. (2004). The mechanism, function and regulation of depolymerizing kinesins during mitosis. Trends Cell Biol. *14*, 537–546.
14. Desai, A., Verma, S., Mitchison, T.J., and Walczak, C.E. (1999). Kin I kinesins are microtubule-destabilizing enzymes. Cell *96*, 69–78.
15. Maney, T., Wagenbach, M., and Wordeman, L. (2001). Molecular dissection of the microtubule depolymerizing activity of mitotic centromere-associated kinesin. J. Biol. Chem. *276*, 34753–34758.
16. Rusan, N.M., Fagerstrom, C.J., Yvon, A.M., and Wadsworth, P. (2001). Cell cycle-dependent changes in microtubule dynamics in living cells expressing green fluorescent protein-alpha tubulin. Mol. Biol. Cell *12*, 971–980.
17. Kline-Smith, S.L., and Walczak, C.E. (2004). Mitotic spindle assembly and chromosome segregation: refocusing on microtubule dynamics. Mol. Cell *15*, 317–327.

18. Joglekar, A.P., and Hunt, A.J. (2002). A simple, mechanistic model for directional instability during mitotic chromosome movements. Biophys. J. *83*, 42–58.
19. Skibbens, R.V., Skeen, V.P., and Salmon, E.D. (1993). Directional instability of kinetochore motility during chromosome congression and segregation in mitotic newt lung cells: A push-pull mechanism. J. Cell Biol. *122*, 859–875.
20. Rieder, C.L., and Salmon, E.D. (1998). The vertebrate cell kinetochore and its roles during mitosis. Trends Cell Biol. *8*, 310–318.
21. Unsworth, A., Masuda, H., Dhut, S., and Toda, T. (2008). Fission yeast kinesin-8 Klp5 and Klp6 are interdependent for mitotic nuclear retention and required for proper microtubule dynamics. Mol. Biol. Cell *19*, 5104–5115.
22. Tischer, C., Brunner, D., and Dogterom, M. (2009). Force- and kinesin-8-dependent effects in the spatial regulation of fission yeast microtubule dynamics. Mol. Syst. Biol. *5*, 250.
23. Bringmann, H., Skiniotis, G., Spilker, A., Kandels-Lewis, S., Vernos, I., and Surrey, T. (2004). A kinesin-like motor inhibits microtubule dynamic instability. Science *303*, 1519–1522.